Amplification of Beam Acceleration in a Plasma by Plasma Instability

V. A. Lebedev

Jeff. Lab

12000 Jefferson Ave., Newport News, VA 23606, USA.

Abstract. Although achieving of high accelerating field in a plasma has been demonstrated experimentally, a practical use of such a scheme for building a large accelerator is questionable. A novel scheme of beam acceleration by a plasma wave is considered in this article. The scheme is based on an initial excitation of a plasma wave by a probe beam with comparatively modest intensity. This seed excitation is then amplified by plasma instability, so that the test beam which follows the probe beam with a small delay will be accelerated by the plasma wave with an amplitude significantly exceeding the initial amplitude of the wave. Because of small interaction between the synchronization beam and the plasma, such a scheme allows one to excite a plasma over large length and, consequently, to build a large accelerator.

INTRODUCTION

Beam acceleration by plasma wave first suggested in reference (1) has created new horizons in achieving high accelerating gradients in linear accelerators. In comparison with a general linear accelerator based on an electromagnetic wave propagated in a waveguide, it allows one to reach an order of magnitude higher accelerating gradient of about 1 GeV/m. Achieving such high gradients has been recently demonstrated experimentally by a few groups (2, 3), but many technical and scientific problems have to be resolved before such an accelerator can be built.

Plasma acceleration has a serious advantage in comparison with classical accelerators: it does not involve high electromagnetic fields on vacuum chamber walls and therefore does not have a problem of high voltage breakup. In general, the plasma accelerator is based on plasma excitation by an intense laser (1) or electron (4) pulse. We will call this the probe bunch. Then, after a short delay, when the amplitude of the plasma wave reaches the maximum, the accelerated bunch is injected. We will call that the test bunch. While creating the initial plasma does not represent great difficulties, both electron and plasma excitations have the common problem of creating a sufficiently intense probe bunch. To resolve this problem one needs to reduce the amount of energy pumped into the plasma, which requires a smaller electromagnetic field volume and, consequently, smaller wavelength.

There is another basic reason pushing us to smaller wavelength. It is determined by properties of the plasma oscillations. To make an estimate we consider the flat plasma wave propagating with phase velocity equal to the light velocity, c, in a boundless plasma. For simplicity we will use non-relativistic formulas. In this case from the

DOE # ——

equations $\operatorname{div}\mathbf{E} = 4\pi n$ and $m\dot{\mathrm{v}} = e\mathbf{E}$ one can deduce that the electric field amplitude is $E_{\max} = 4\pi e n_e \xi / k$, while the amplitude of the electron velocity oscillations is $\tilde{\mathrm{v}} = eE_{\max} / m\omega$. Here n_e is the electron density, e is the electron electric charge, ξ is the relative density perturbation, $\xi = \Delta n_e / n_e$, and k is the wave vector[1]. Taking into account that $k = \omega / c$, the oscillation frequency is equal to the plasma frequency, $\omega_p = \sqrt{4\pi n_e e^2 / m}$, and expressing values through ξ and the wavelength, $\lambda = 2\pi / k$, one obtains

$$\tilde{\mathrm{v}} = c\xi \quad , \qquad E_{\max} = \frac{2\pi m c^2 \xi}{e\lambda} \quad . \tag{1}$$

The first equation shows that the large relative density perturbation, ξ, yields relativistic motion of plasma electrons, and thus additionally increases the motion non-linearity, which limits ξ to about $\xi \le 0.1$. The second equation can be rewritten in practical units as follows, $\lambda_{[\mathrm{mm}]} = 3.21\xi / E_{\max[\mathrm{GeV/m}]}$, that for $E_{\max} = 1$ GeV/m and $\xi = 0.1$ yields λ=0.32 mm.

Practical use of so small wavelength in a high-energy accelerator creates two fundamental problems. First, how one can phase the accelerating voltage of different accelerator sections. Second, how one can suppress harmful focusing effects due to transverse components of the accelerating field. The second issue is additionally complicated by the fact that the focusing effects are different along the accelerating bunch. The accelerating scheme considered in this article addresses these two issues as well as how to excite the plasma wave without creating a very intense probe bunch.

The main problems of the considered before schemes arise from the fact that the probe test bunch performs two functions. It carries the energy for plasma excitation and it excites and synchronizes the plasma wave. It can work well for a small accelerator, but with increased accelerator size it will require thousands of intense high-energy probe bunches for plasma excitation. This makes an accelerator too expensive and therefore unrealistic. To resolve the question of section synchronization one needs to separate these two functions. The basic idea is in the following. One creates an unstable plasma but before the instability has developed, a low-intensity probe bunch is injected, making a seed excitation. The probe bunch excites many modes, but the plasma only amplifies the mode with the correct field configuration, thus creating a high-quality accelerating wave. After the amplitude of the plasma wave reaches the maximum, the test bunch is injected for acceleration. To create the required plasma properties it is immersed into a longitudinal magnetic field.

To formulate the main requirements for such plasma acceleration we will start our consideration from basic low frequency analysis of plasma properties when the vertex part of the electromagnetic field is omitted (Section 1). This model is comparatively

[1] To simplify formulas I will use the SGS system through the article.

simple and well describes waves with phase velocities less than light velocity. Then, we will discuss a two-beam instability as a candidate to make the plasma unstable (Section 2). Finally, we will consider possible parameters of the suggested accelerator (Section 3).

1. LONGITUDINAL WAVES IN PLASMA COLUMN

Let's consider a plasma column with radius a inside a vacuum chamber with radius b as shown in figure 1. Neutral plasma has a uniform density distribution across the column and is immersed into longitudinal magnetic field B_0. The electron density n_e and the ion density n_i satisfy to the neutrality condition, $\sum_i Z_i n_i - n_e \equiv \sum_\alpha Z_\alpha n_\alpha = 0$. The motion of the electrons and ions in such a system is described by the following system of equations:

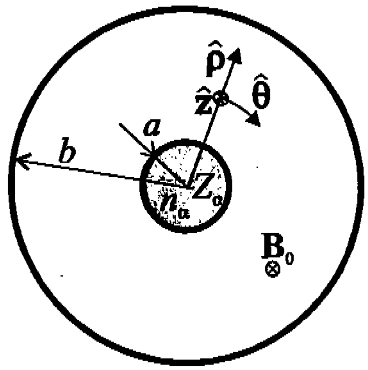

FIGURE 1. Coordinate frame and plasma column layout.

$$\frac{\partial \mathbf{v}_\alpha}{\partial t} + \left(\mathbf{v}_\alpha, \frac{\partial}{\partial \mathbf{x}}\right)\mathbf{v}_\alpha = \frac{Z_\alpha e}{m}\left(-\nabla\varphi + \frac{\mathbf{v}_\alpha \times \mathbf{B}_0}{c}\right) \quad ,$$
$$\frac{\partial n_\alpha}{\partial t} + div(n_\alpha \mathbf{v}_\alpha) = 0 \quad , \qquad (2)$$
$$\Delta\varphi = -4\pi e \sum_\alpha Z_\alpha n_\alpha \quad .$$

Linearizing these equations and looking for an axial symmetric solution,

$$\begin{vmatrix} \mathbf{v}(r,z,\theta,t) \\ n_\alpha(r,z,\theta,t) \\ \varphi(r,z,\theta,t) \end{vmatrix} = \begin{vmatrix} \mathbf{v}(r) \\ n_\alpha(r) \\ \varphi(r) \end{vmatrix} e^{i(\omega t - kz)} \quad , \qquad (3)$$

one obtains (see Ref. (5)) the dispersion equation

$$f(k,\omega) \equiv \sqrt{-\varepsilon_\perp(\omega)\varepsilon_\parallel(\omega)}\,\frac{\mathrm{J}_1\left(ka\sqrt{-\frac{\varepsilon_\parallel(\omega)}{\varepsilon_\perp(\omega)}}\right)}{\mathrm{J}_0\left(ka\sqrt{-\frac{\varepsilon_\parallel(\omega)}{\varepsilon_\perp(\omega)}}\right)} - \frac{\mathrm{I}_1(ka)\mathrm{K}_0(kb) + \mathrm{I}_0(kb)\mathrm{K}_1(ka)}{\mathrm{I}_0(kb)\mathrm{K}_0(ka) - \mathrm{I}_0(ka)\mathrm{K}_0(kb)} = 0 \quad .(4)$$

Here $J_0(x)$ and $J_1(x)$ are the Bessel functions, $I_0(x)$, $I_1(x)$, $K_0(x)$ and $K_1(x)$ are the modified Bessel functions, $\varepsilon_{\|}(\omega)$ and $\varepsilon_{\perp}(\omega)$ are the longitudinal and transverse plasma dielectric permittivities,

$$\varepsilon_{\|}(\omega) = 1 - \frac{1}{\omega^2}\sum_{\alpha}\omega_{p_\alpha}{}^2 \quad ,$$
$$\varepsilon_{\perp}(\omega) = 1 - \sum_{\alpha}\frac{\omega_{p_\alpha}{}^2}{\omega^2 - \Omega_\alpha{}^2} \quad , \tag{5}$$

and ω_{p_α} and Ω_α are the plasma and Larmor frequencies,

$$\omega_{p_\alpha} = \sqrt{\frac{4\pi n_\alpha Z_\alpha{}^2 e^2}{m_\alpha}} \quad ,$$
$$\Omega_\alpha = \frac{eZ_\alpha B_0}{m_\alpha c} \quad . \tag{6}$$

Only fast plasma oscillations, related to electrons, are important for the instability considered below, and therefore we will eliminate below the ion contribution into the dielectric permittivities, leaving only the electron contribution with the electron plasma frequency ω_{pe} and electron Larmor frequency Ω_e.

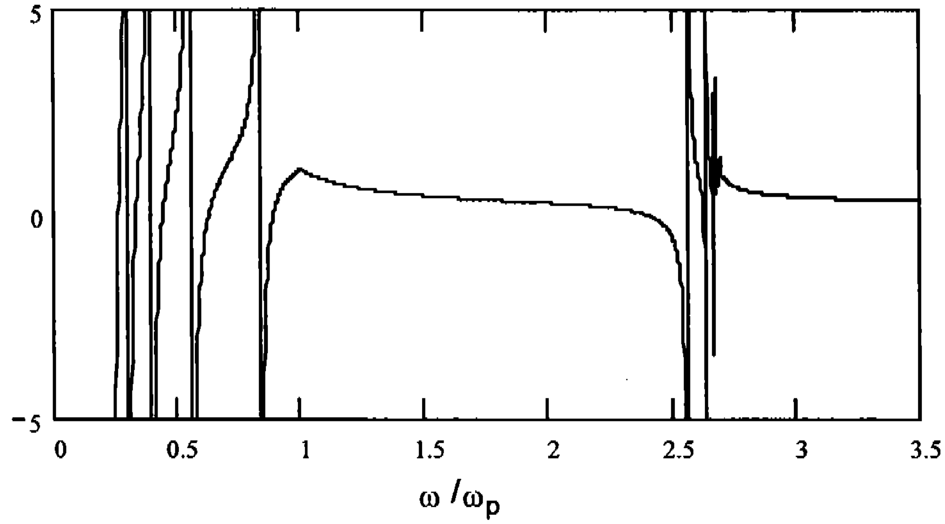

FIGURE 2. Function $f(k,\omega)$ of equation (4) as function ω for $ka = 4$, $b/a = 5$ and Ω_e/ω_{pe}=2.5.

Equation (4) cannot be solved analytically and therefore its solutions were studied numerically. For every given k this equation has an infinite number of roots corresponding to a different number of potential variations as a function of radius. As will be seen below we are interested in the case of a sufficiently strong magnetic field and therefore, to simplify further analysis, we will consider below a plasma where $\Omega_e > \omega_{pe}$. In this case there are two well-separated groups of roots, as illustrated in figure 2 by a plot of function $f(k,\omega)$. The first group is at low frequencies. Its roots belong to the solutions with primarily longitudinal motion of the electrons. They are grouped near the frequency where $\varepsilon_{\|}(\omega)$ approaches infinity, ω=0. The second group is at high frequencies. These roots belong to the solutions with primarily transverse motion of the electrons. The roots are grouped around the frequency where $\varepsilon_{\perp}(\omega)$ approaches zero, $\omega = \sqrt{\omega_{pe}^2 + \Omega_e^2}$. To produce a clear picture only the first few roots from both groups are shown in figure 2. We denote roots using two numbers, like $\omega_{0,2}$. The first number, equal to 0 or 1, denotes the group number, and the second number denotes the number of potential variations – the number of zero crossings by potential dependence on radius. Note that when the sign of function $\varepsilon_{\|}(\omega) / \varepsilon_{\perp}(\omega)$ becomes positive the argument in Bessel functions becomes imaginary and they need to be replaced by the modified Bessel functions. This transformation was used for plotting the curve in figure 2.

The solution with zero number of variations in the first group has highest frequency among all other roots in the group. Its asymptotic for the case of long waves, $ka \ll 1$, is

$$\omega_{0,0}(k) = \omega_{pe} ka \sqrt{\frac{\ln(b/a)}{2}} \quad , \tag{7}$$

showing that this mode has linear dispersion and consequently constant phase velocity

$$v_{\phi 0} = \omega_{pe} a \sqrt{\frac{\ln(b/a)}{2}} \quad . \tag{8}$$

In the case of short waves, $ka \gg 1$, the asymptotic can be easily obtained for the cases of small and high magnetic field,

$$\omega_{0,0}(k) = \begin{cases} \omega_{pe}/\sqrt{2} & , \quad \Omega_e \ll \omega_{pe} \quad , \\ \omega_{pe} & , \quad \Omega_e \gg \omega_{pe} \quad . \end{cases} \tag{9}$$

Asymptotics for intermediate values of the magnetic field lie between these two values.

In the second group the solution with zero number of variations has the lowest frequency among all other roots in the group. Its asymptotics for the cases of long and short waves are

$$\omega_{1,0} = \begin{cases} \sqrt{\omega_{pe}^{\ 2} + \Omega_e^{\ 2}} & , \quad ka \ll 1 \ , \\ \sqrt{\dfrac{\omega_{pe}^{\ 2} + \Omega_e^{\ 2}}{2}} & , \quad kb \gg 1 \ . \end{cases} \tag{10}$$

Solutions with higher number of variations have the same asymptotic at small wavelength, while for short wavelength asymptotics, they are in the range of $\left[\Omega_e, \sqrt{\Omega_e^{\ 2} + \omega_{pe}^{\ 2}}\right]$.

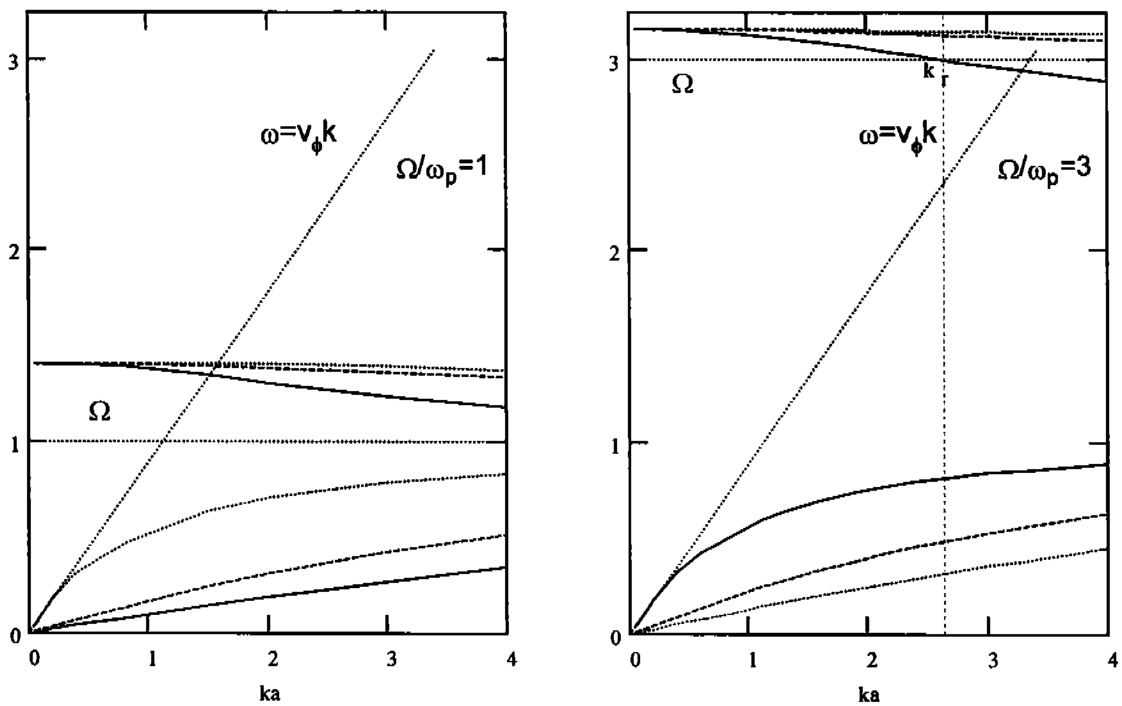

FIGURE 3. Dispersion curves for the first three modes of both low (bottom three curves in both pictures) and high (top three curves in both pictures) frequency groups; left picture - Ω_e/ω_{pe}=1.0, right picture - Ω_e/ω_{pe}=3.0.

Figure 3 illustrates behavior of the dispersion curves for the cases of small and high magnetic fields. Dispersion curves for solutions with zero, one, and two variations for both high and low frequency groups are shown. One can see that the magnetic field does not significantly affect curves belonging to the low frequency group, while it significantly changes the curves of the high frequency group.

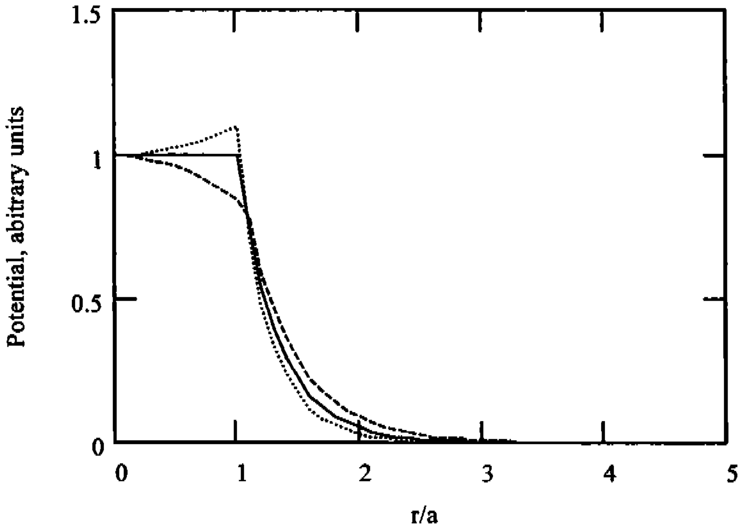

FIGURE 4. Dependence of potential on radius in vicinity and at resonance; b/a = 5 and Ω/ω_p=3; solid line - $\omega/\omega_p = 3$, $ka = 2.64$, dotted line - $\omega/\omega_p = 3.048$, $ka = 2.12$, dashed line - $\omega/\omega_p = 2.953$, $ka = 2.12$

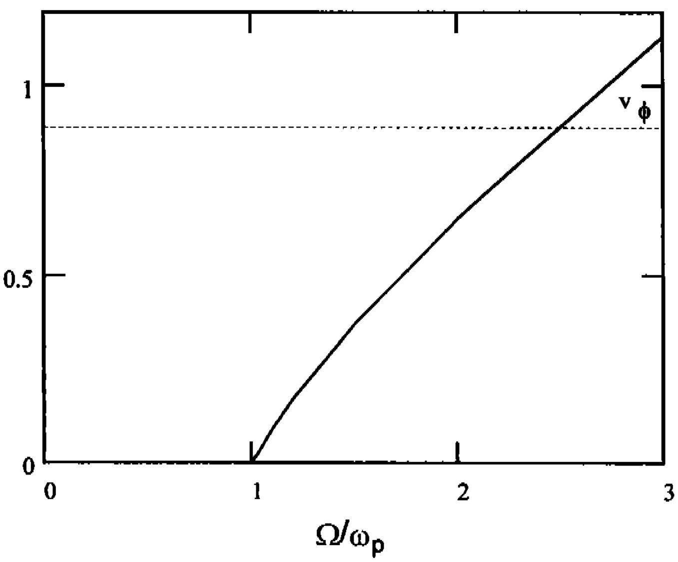

FIGURE 5. Dependence of the wave phase velocity (in units of $\omega/(\omega_p ka)$) at resonance ($\omega_{1,0} = \Omega$) as a function of ratio Ω/ω_p.; $b/a = 5$.

Dependence of the potential on the radius is determined by the value of $\varepsilon_{\parallel}(\omega)/\varepsilon_{\perp}(\omega)$ at corresponding eigen-frequency, $\omega_{m,n}(k)$. If $\varepsilon_{\parallel}(\omega)/\varepsilon_{\perp}(\omega)$ is negative the potential is

$$\varphi(r,z,t) = \varphi_0 \, \mathrm{J}_0\left(ka\sqrt{-\frac{\varepsilon_{\|}(\omega_{m,n}(k))}{\varepsilon_{\perp}(\omega_{m,n}(k))}} \right) e^{i(\omega t - kz)} \quad . \tag{11}$$

For the positive value the Bessel function in equation (11) has to be replaced by the modified Bessel function $\mathrm{I}_0(x)$. As can be seen from figure 3, the high frequency zero variation root $\omega_{1,0}$ crosses frequency line $\omega = \Omega_e$ where the transverse dielectric permittivity approaches infinity. At this point, $\omega_{1,0}(k_r) = \Omega$, and the dependence of the potential on the radius inside the plasma vanishes, creating an ideal longitudinal accelerating wave, which does not have a transverse electric field and for which acceleration does not depend on radius. The dependencies of potential on radius for the resonance wave vector, k_r, and for 20% longer and shorter wavelengths are shown in figure 4. Figure 5 depicts the dependence of the phase velocity at resonance as a function of the ratio Ω/ω_p. For frequency $\Omega/\omega_p < 1$ the resonance condition cannot be fulfilled. Note that the phase velocity at resonance is higher than the phase velocity of the low frequency plasma wave (see equation 8) for $\Omega/\omega_p > 2.51$.

2. TWO-BEAM INSTABILITY

The probe beam excites many small amplitude modes in the plasma. To create a good-quality accelerating wave from this seed excitation only one mode with correct structure and phase velocity has to be amplified. In our study we will analyze the two-beam instability as a candidate to amplify the beam acceleration in the plasma.

To simplify formulas we will consider a simple model where a non-relativistic electron beam propagates along the plasma column. The beam has the same radius as plasma and its velocity is v_0. The beam density, n_b, is uniform and is much smaller than the electron density in the plasma, n_p. The low density of the beam allows one to consider this system as a neutral plasma, and therefore the dispersion properties of such a system are described by the same equation (4) as properties of the plasma column. But the beam permittivities of equation (5) have to be corrected to take into account the electron beam motion,

$$\begin{aligned} \varepsilon_{\|}(\omega) &= 1 - \frac{\omega_{pe}^{\;2}}{\omega^2} - \frac{\omega_{pb}^{\;2}}{(\omega - k\mathrm{v})^2} \quad , \\ \varepsilon_{\perp}(\omega) &= 1 - \frac{\omega_{pe}^{\;2}}{\omega^2 - \Omega_e^{\;2}} - \frac{\omega_{pb}^{\;2}}{(\omega - k\mathrm{v})^2 - \Omega_e^{\;2}} \quad , \end{aligned} \tag{12}$$

where ω_{pe} and ω_{pb} are the plasma the frequencies related, correspondingly, to electrons of the plasma and the beam, and v is the electron beam velocity.

In the first approximation one can consider the plasma and the beam independent so that waves propagating in the plasma and in the beam do not interact with each other. The general instability criterion states that the instability can develop if the phase velocities of waves related to the plasma and to the beam are equal. Because of low electron density in the beam, the phase velocity of the plasma wave related to the beam is much smaller than the velocity of the beam and we can simplify the criterion comparing the wave phase velocity and the electron beam velocity. First, we want to avoid an instability at low frequencies. This implies that the electron beam velocity has to be higher than the phase velocities of the low frequency plasma waves, $v > v_{\phi 0}$. Second, we would like to excite a resonant wave considered above where the transverse dielectric permittivity approaches infinity and the transverse electric field vanishes. As can be seen from figure 5, this requires a strong magnetic field so that $\Omega/\omega_p > 2.51$.

The rest of this section will be devoted to study of properties of the resonant wave. To find the instability increment we will rewrite equation (4) in the following form

$$\frac{J_1\left(ka\sqrt{-\frac{\varepsilon_\parallel(\omega)}{\varepsilon_\perp(\omega)}}\right)}{J_0\left(ka\sqrt{-\frac{\varepsilon_\parallel(\omega)}{\varepsilon_\perp(\omega)}}\right)}=\frac{1}{\sqrt{-\varepsilon_\perp(\omega)\varepsilon_\parallel(\omega)}}\frac{I_1(ka)K_0(kb)+I_0(kb)K_1(ka)}{I_0(kb)K_0(ka)-I_0(ka)K_0(kb)} \quad . \tag{13}$$

One can see that if $\varepsilon_\perp(\omega)$ approaches infinity the expression in the right-hand side approaches zero and consequently Bessel functions at the left-hand side can be expended in Taylor series, $J_1(z)/J_0(z) = z/2 + \ldots$, yielding the following equation:

$$\varepsilon_\parallel(\omega)+\frac{1}{ka}\frac{I_1(ka)K_0(kb)+I_0(kb)K_1(ka)}{I_0(kb)K_0(ka)-I_0(ka)K_0(kb)}=0 \quad . \tag{14}$$

Substituting $\varepsilon_\parallel(\omega)$ from equation (12) and expending the obtained equation in Taylor series near the resonance we obtain

$$\frac{\delta}{(x-y-u)^2}-\frac{2\omega_p^{\ 3}}{\Omega^3}x-\frac{2\omega_p}{\Omega k_r a}\left(f(k_r)-\left.\frac{df}{dk}\right|_{k=k_r}k_r\right)y=0 \quad . \tag{15}$$

Here we took into account that at the resonance, $\omega = \Omega$,

$$\frac{\omega_p^{\ 2}}{\Omega^2}-1=\frac{2}{k_r a}f(k_r) \quad , \tag{16}$$

and we denoted

$$f(k)=\frac{\mathrm{I}_1(ka)\mathrm{K}_0(kb)+\mathrm{I}_0(kb)\mathrm{K}_1(ka)}{\mathrm{I}_0(kb)\mathrm{K}_0(ka)-\mathrm{I}_0(ka)\mathrm{K}_0(kb)} \quad ,$$

$$\omega=\Omega+\omega_p x \quad , \qquad k=k_r+\frac{\omega_p}{\mathrm{v}_0}y \quad , \quad \mathrm{v}_0=\frac{\Omega}{k_r} \tag{17}$$

$$\delta=\frac{\omega_b^{\;2}}{\omega_p^{\;2}}\equiv\frac{n_b}{n_e} \quad , \qquad \mathrm{v}=\mathrm{v}_0+\frac{\omega_p}{k_r}u \quad .$$

Equation (15) is the cubic equation relative to the variable x (dimensionless frequency deviation from resonance value of Ω) as a function of y (dimensionless wave vector deviation from resonance value of k_r) and u (dimensionless deviation of the beam velocity from the resonance velocity v_0). At resonance, $y = u = 0$, and equation (15) yields the increment equal to

$$\lambda_{\max}=\mathrm{Im}(\omega)=\omega_p\,\mathrm{Im}(x)=\frac{\sqrt{3}}{2\cdot 2^{1/3}}\Omega\delta^{1/3} \quad . \tag{18}$$

Numerical analysis of the roots of equation (15) exhibited that the maximum value of the instability increment is achieved at resonance. Dependence of the real and imaginary parts of equation 15 roots for $\delta = 0.001$ is shown in figure 6. The instability increment is proportional to the imaginary part of a root, $\lambda = \omega_p\mathrm{Im}(x)$, while frequency is determined by its real part, $\omega = \Omega + \omega_p\mathrm{Re}(x)$. The width of the amplification band is characterized by

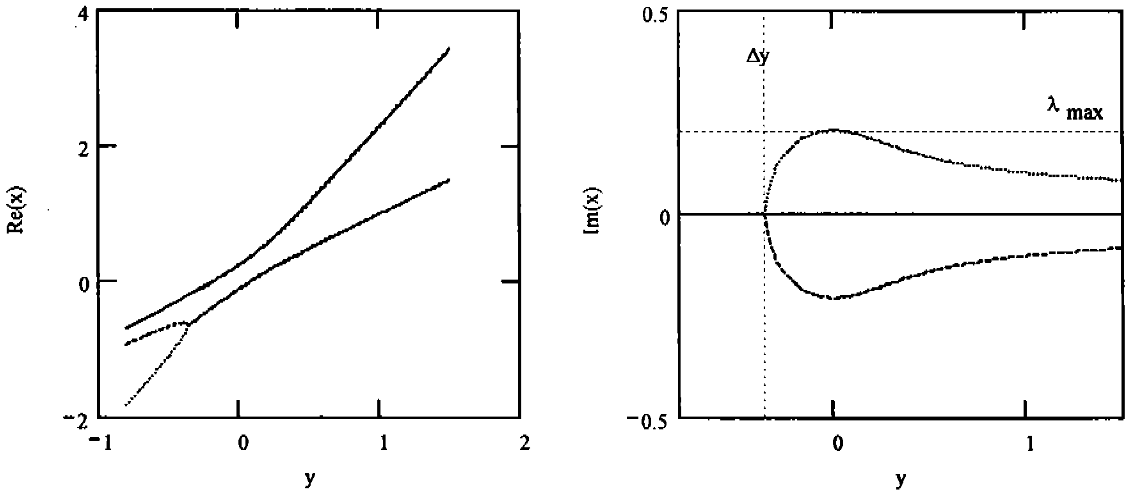

FIGURE 6. Dependence of the roots of equation (15) on the dimensionless wave vector y; $\Omega/\omega_p = 3$, $\delta = 0.001$, $b/a = 5$, $u = 0$.

$$\Delta k = \frac{\omega_p}{v_0}\Delta y \cong \frac{3\Omega\delta^{1/3}}{2v_0\left(1+\frac{\Omega^2}{\omega_p{}^2 k_r a}\left(f(k_r)-\left.\frac{df}{dk}\right|_{k=k_r} k_r\right)\right)} \quad . \tag{19}$$

Numerical analysis also proved that the maximum increment and the bandwidth do not depend significantly on a small change of the electron beam velocity

It is important to note that presence of the electron beam changes also the group velocity of the plasma wave in the vicinity of resonance. Without the electron beam, as can be seen from figure 3, the group velocity, $d\omega_{10}/dk \approx -0.1\cdot v_0$, is negative, while the group velocity of the same mode is positive $d\omega_{10}/dk \approx 0.5\cdot v$ (see figure 6) in the presence of the beam. Positive group velocity in the whole amplification band implies that this instability is the convective instability, i.e. an initial perturbation grows with time but simultaneously moves downstream together with the electron beam, and therefore the amplitude of the wave does not grow to infinity at any given longitudinal coordinate.

3. ACCELERATOR SECTION PARAMETERS

Utilization of the resonant condition in plasma acceleration addresses three important issues. First, it removes the transverse electric field and thus prevents beam focusing by the accelerating field. Second, it suppresses the dependence of the accelerating field on the transverse coordinates. Third, it reduces the dependence of accelerating frequency on plasma density because the frequency is mainly determined by the magnetic field

$$\omega \approx \Omega\left(1+\omega_{pe}{}^2/\left(2\Omega^2\right)\right) \quad . \tag{20}$$

But realization of this resonant condition requires high Larmor frequency, $\Omega/\omega_p > 2.51$, and, consequently, high magnetic field. For acceleration gradients of about 1 GV/m the field value is beyond or on the boundary of today's state-of-art achievements. For an estimate of the accelerating section parameters (table 1) the magnetic field of 12 T is used.

The choice of instability increment is determined by the accelerating frequency and its achievable accuracy. Picking up an accuracy of plasma density of about 1%, and $\Omega/\omega_p\approx 3$, one obtains from equation (20) the relative accuracy of the accelerating frequency of about $5\cdot 10^{-4}$, which implies that the plasma wave keeps correct phase for about 1000 oscillations. For an accelerating frequency of 340 GHz and amplification of 10 times, one obtains the instability growth time of about 1 ns. This time is significantly less than that required for an electron to pass the accelerating section.

To create such a beam-plasma system the following mechanism is suggested. An electron beam with pulse length of about 50 ns and rise and fall time less than about 10 ns is directed to a vacuum chamber with gas density equal to the required plasma density. We will call this beam the excitation beam. At this time there is no plasma and the system is stable. To create the plasma, immediately after the beam current reaches its flat top a short laser pulse is aimed along the beam. A laser pulse with comparatively modest energy can ionize all gas on its way. Thus the pulse creates a plasma with the required density and makes the system unstable. After a small delay, which is mainly determined by the synchronization accuracy, the probe bunch follows. This bunch makes the seed excitation, which then is amplified by the instability. After the plasma wave amplitude reaches the required value (about 3 ns) the test bunch is accelerated by the plasma wave. This procedure does not require very good synchronization for the excitation and laser pulses, but requires sub-picosecond synchronization for the probe and test bunches, which can be comparatively easily achieved by accelerator means.

Main parameters of the accelerating section are shown in table 1. The parameters were estimated on the basis of the non-relativistic theory considered above with simple corrections taking into account an increase of the longitudinal mass for relativistic electrons. Because of the low intensity of the probe bunch and, consequently, the small energy loss on plasma excitation, the probe bunch can excite a plasma column of rather large length. The length of the acceleration section was chosen to be 10 m, which is mainly determined by engineering matters.

TABLE 1. Parameters of the accelerator section

Accelerating gradient	0.2 GeV/m
Wave length of the RF	0.89 mm
Section length	10 m
Plasma (electron beam) diameter	0.75 mm
Magnetic field	12 T
Plasma density	$1.6\cdot10^{14}$
Energy in plasma per unit length at max. field	74 mJ/m
Plasma frequency, $\omega_p/2\pi$	112 GHz
Instability increment	$1\cdot10^{9}$ s
Energy of the excitation electron beam	2 MeV
Current of the excitation electron beam	200 A
Density of the excitation electron beam	$5.4\cdot10^{12}$
Energy in electron beam per unit length	1.4 J/m
Energy in ionization laser pulse	5 mJ
Ionization laser wave length	300 nm
Number of particles in excitation bunch	$1.1\cdot10^{8}$
Rms bunch length	50 μm

CONCLUSION

The novel scheme of plasma acceleration considered above is based on the narrow band instability in a plasma. It allows one to choose and amplify only one of many modes excited by the probe beam in the plasma, and, consequently, it allows one to form a well-defined accelerating wave. The scheme has been illustrated by non-relativistic analysis of the two-beam instability. This analysis showed a possible way of carrying out such a scheme for non-ultra-relativistic particles. In particular it can be considered for acceleration of heavy ions in the energy range of 1–6 GeV/nucleon while more studies are required to make a realistic scheme. Further study is required for developing a similar scheme for acceleration of ultra-relativistic particles.

ACKNOWLEDGEMENTS

I would like to thank S. Corneliussen for his help in this article editing.

REFERENCES

1. T. Tajima and J.M. Dowson, Phys. Rev. Lett. **43**, 267 (1979).
2. Y. Kitogawa *et al.*, Phys. Rev. Lett. **68**, 48 (1992).
3. *Advanced Accelerator Concepts*, edited by J. S. Wurtele, AIP Conf. Proc. No. 279 (AIP, New York, 1993).
4. P. Chen, J. M. Dawson, R. W. Huff and T. Katsouleas, Phys. Rev. Lett. **54**, 693 (1985).
5. R. C. Davidson, *Theory of nonneutral plasmas*, Addison-Wesley Publishing Coompany, Inc., 1988, ch. 2.7, pp. 45-49.